2015 ACRS THE 36TH ASIAN CONFERENCE ON REMOTE SENSING
FOSTERING RESILIENT GROWTH IN ASIA
QUEZON CITY, METRO MANILA PHILIPPINES

LANDCOVER CLASSIFICATION OF HYPERSPECTRAL IMAGES

A.Munkh-Erdene[1] and M.Ganzorig

Institute of Geography and Geoecology[1], Mongolian Academy of Sciences
Ave.Enkhtaivan-54B, Ulaanbaatar-51, Mongolia;
Tel: 976-11-453660, Fax: 976-11-458090
E-mail: munkherdene@informatic.ac.mn
E-mail: ganzorig@arvis.ac.mn

KEY WORDS: Hyperspectral remote sensing, PCA, land cover

ABSTRACT: In recent years, the processing and analysis of hyperspectral images have become the main tasks of many researchers dealing with RS image processing. Unlike the traditional multispectral datasets taken in the optical range of electro-magnetic spectrum, the hyperspectral data deals with an enormous amount of bands and the data are formed as collections of hundreds of images of the same scene with each image corresponding to a narrow interval of the electro-magnetic wavelength. It is clear that such datasets offer the superior potential for more accurate and detailed information extraction than is possible with other types of RS data. The purpose of this paper is to classify landcover using hyperspectral images. For the feature extraction, principal average of visible, near infrared and mid infrared bands, assorting of high correlation bands and component transformation (PCA) have been applied. Advanced satellite images classification represents an accurate and cost effective for land cover mapping at regional scale. The output of each of the feature extraction method is classified using a maximum likelihood classification method. The results are analyzed and compared.

1. INTRODUCTION

Over the years, on the remote sensing research using hyperspectral data create many advantages. Unlike the traditional multispectral datasets taken in the optical range of electro-magnetic spectrum, the hyperspectral data deals with an enormous amount of bands and the data are formed as collections of hundreds of images of the same scene with each image corresponding to a narrow interval of the electro-magnetic wavelength. It is clear that such datasets offer the superior potential for more accurate and detailed information extraction than is possible with other types of RS data. This means that hyperspectral data sets provide a wealth of information and are used for many different applications such as geological investigation, forest change analysis, environmental mapping, global change study, wetlands mapping, crop analysis, traffic ability assessment, plant identification, mineral recognition, and many others (Plaza *et al.* 2012, Amarsaikhan *et al.* 2011).

As the hyperspectral images consist of a large number of bands, their unique characteristics pose different processing problems, which could be necessarily tackled under specific mathematical formalisms, such as segmentation and classification as well as spectral mixture analysis (Smith *et al.* 1990 and Jia *et al.* 1999). In order to reduce the data volume, the techniques for reducing the image dimensionality are often applied. Usually, it is reduced by applying different transformation techniques by retaining only the significant components for further processing. Information extraction is generally done through classification of the images and identifies which pixels contain a variety of spectrally distinct labels. Many attempts are being made to reduce the data dimensionality and extract reliable information needed for different decision-making (Amarsaikhan and Ganzorig 1999, Keshava and Mustard 2002, Richards 2005, Tsai *et al.* 2009, Yang *et al.* 2009, Vega *et al.* 2012).

The aim of this research is to classify landcover using hyperspectral images. In this study, Hyperspectral Imager (Hyperion) onboard EO-1 satellite sensor images have been used, Hyperion, which acquires data in 242 bands, 10-nanometer-wide bands from 0.4 to 2.6 micrometers (USGS, 2005). For the feature extraction, principal average of visible, near infrared and mid infrared bands, assorting of high correlation bands and component transformation (PCA) have been applied. Advanced satellite images classification represents an accurate and cost effective for land cover mapping at regional scale. The output of each of the feature extraction method is classified using a maximum likelihood classification method. The results are analyzed and compared.

2. METHODOLOGY

Before the land cover classification using Hyperion sensor images, the data dimensionality should be reduced and feature extraction is needed, for this purpose following three type of methods have been recommended:

I. Compress data instantaneously using principal component transformation
II. Segmentation of high correlation bands and compress data
III. Define principal average of visible, near infrared and mid infrared bands and compress

I. Data dimensionality compression and feature extraction using principal component transformation (PCT). The PCT is a statistical technique that transforms a multivariate data set of intercorrelated variables into a set of new uncorrelated linear combinations of the original variables, thus generating a new set of orthogonal axes (Richards and Xia, 1999). It is also a data compression technique used to reduce the dimensionality of the multidimensional datasets and helpful for image encoding, enhancement and multitemporal dimensionality (Pohl and Van Genderen 1998).

II. Before the data compression compute statistics and define correlation coefficients are needed. A correlation coefficient is meaning statistical relationships between two or more random variables and observed data values (Amarsaikhan, 2008). A correlation coefficient *r* is:

$$r_{x,y} = \frac{n\sum_{i=1}^{n} x_i y_i - \sum_{i=1}^{n} x_i \sum_{i=1}^{n} y_i}{\sqrt{n\sum_{i=1}^{n} x_i^2 - \left(\sum_{i=1}^{n} x_i\right)^2}\sqrt{n\sum_{i=1}^{n} y_i^2 - \left(\sum_{i=1}^{n} y_i\right)^2}} \quad (1)$$

The value of correlation coefficient *r* is such that -1<0<+1. If *r* value is close to +1 positive correlation, if opposite negative correlation. After defining correlation coefficient of the hyperspectral bands to cluster higher correlation bands and compress data using principal component transformation.

III. Initially, to define principal average of the hyperspectral bands based on characteristic of electromagnetic spectrum radiation interaction with natural or human built objects, for instance clustering visible, near infrared and mid infrared bands (formula 2). Hereon, to compress data using principal component transformation.

$$
\begin{aligned}
Ave\_visible &= \sum_{i=8}^{36} bi / 28 \\
Ave\_NIR &= \sum_{i=36}^{96} bi / 61 \\
Ave\_MIR1 &= \sum_{i=96}^{150} bi / 54 \\
Ave\_MIR2 &= \sum_{i=150}^{220} bi / 70
\end{aligned} \tag{2}
$$

In this study, after data compression, for the actual classification, maximum likelihood classification method has been used for land cover classification. The maximum likelihood classification is the most widely used statistical classification technique, because a pixel classified by this method has the maximum probability of correct assignment (Amarsaikhan *et al.* 2011).

3. RESULTS

In the current study, Hyperion data taken on 30 October 2005, have been used. Initially, the multi-channel Hyperion image has been analyzed in terms of radiometric quality. It was found out that the water absorption bands and some other bands of the image had zero values. When these 67 bands have been excluded, the original Hyperion dataset was reduced from 242 bands to 175 bands. As a test site, some part of Khan-Bogd soum of Umnugovi province has been selected in Mongolia. Area of interest extends from the south to north 6.7 km and from west to east 6 km, shown in Figure 1a.

I. Principal component transformation (PCT) has been performed using all available bands and the result showed that the first five principal component (PC) contained 97.6% of the overall variance. The visual inspection of a PC6 that contained only 0.4% of the overall variance, indicated that it contained noise. Likewise, the other PCs contained noise from the total data set. A pseudo colour image created by the use of the first three PCs is shown in Figure 1b.
II. Before the data compression correlation coefficients have been defined (see table 1). After defining correlation coefficients, higher correlation bands have been assorted following groups: Group 1: band 8-34, Group 2: band 40-100, Group 3: band 101-150, Group 4: band 151-220. Then PCT has performed all group bands, and a pseudo color image is shown in Figure 1c.

Table 1. Correlation coefficients of clustering bands

bands	**4**	**...**	**39**	**40**	**...**	**100**	**112**	**...**	**151**	**170**	**...**	**220**
4	1	...	.92	.89	...	.84	.82	...	.80	.81	...	.78
...	...	1	...	...	...	...	...	...	...	...	...	...
39	.92	...	1	.98	...	.91	.90	...	.87	.85	...	.82
40	.89	...	.98	1	...	.92	.90	...	.87	.84	...	.83
...	...	...	...	...	1	...	...	...	...	...	...	...
100	.84	...	.91	.92	...	1	.97	...	.94	.93	...	.92
112	.82	...	.90	.90	...	.97	1	...	.95	.92	...	.90
...	...	...	...	...	...	...	...	1	...	...	...	...
151	.80	...	.87	.87	...	.94	.95	...	1	.93	...	.92

170	.81	...	.85	.84	...	.93	.92	...	.93	1	...	.98
...	...	...	...	...	...	...	...	...	...	...	1	...
220	.78	...	.82	.83	...	.92	.90	...	.92	.98	...	1

III. Firstly, the principal average of visible, near infrared and mid infrared bands have been defined, then principal component transformation has performed to the each band groups respectively. Figure 1d shows color image created by the band transformation results.

Classification of the features

Initially, we have to select the training signatures from the area of interest, therefore five classes (dirt road area, bedrock, soil, bare soil, mining area) have been selected from the hyperspectral image, the signatures contain 49-545 pixels. In this study, after three type of data compression, maximum likelihood classification method has been used for land cover classification. Figure 2 shows maximum likelihood classification results. For the accuracy assessment of the classification results, the overall performance has been used. This approach creates a confusion matrix in which reference pixels are compared with the classified pixels and as a result an accuracy report is generated indicating the percentages of the overall accuracy (Amarsaikhan *et al.* 2011). As ground truth information, different AOIs containing 1064 purest pixels have been selected. The overall classification accuracies for the selected areas were 81.86% for the PC bands, 81.67% for the clustering of high correlation bands and 74.43% for the defined average of the bands.

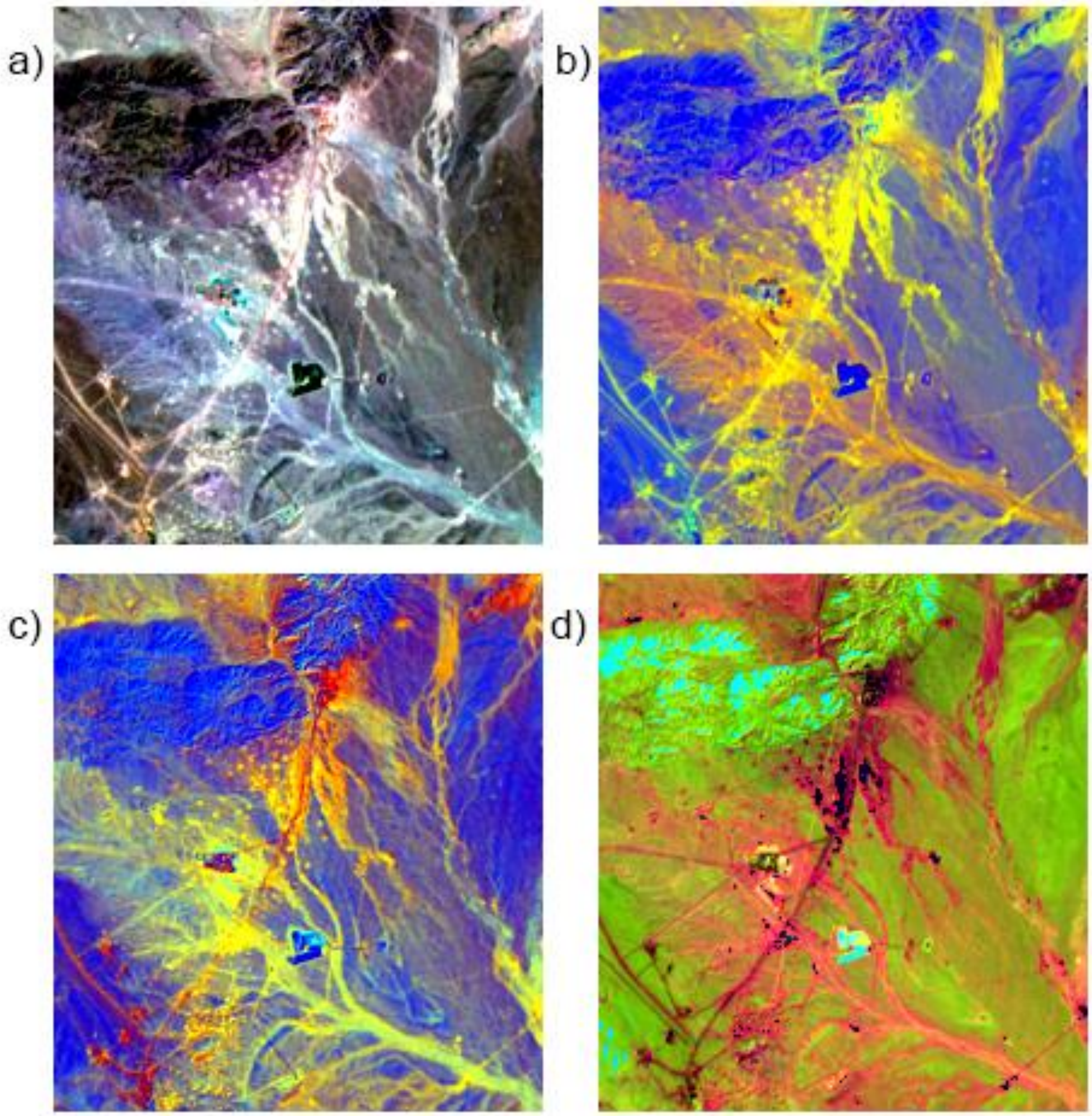

Figure 1. a) Image created by the use of bands 24, 53, 143 b) Image created by the PCT method
c) Image created by high correlation bands clustering d) Image created by defined average of the bands

4. CONCLUSION

The purpose of this paper was to use hyperspectral data for the land cover classification. Before the classification due to reduce the data dimensionality and feature extraction, 1) PCT, 2) segmentation of high correlated bands and 3) defining average of visible, near, mid infrared bands were performed. For the actual classification in this study maximum likelihood supervised classification was performed to each output images respectively. As could be seen from the classification results, using PC bands produced superior result in comparison with other approaches. Therefore, thorough analysis of the HYPERION image indicated that hyperspectral images could be used for an improved land cover mapping and differentiation of the classes having similar spectral characteristics.

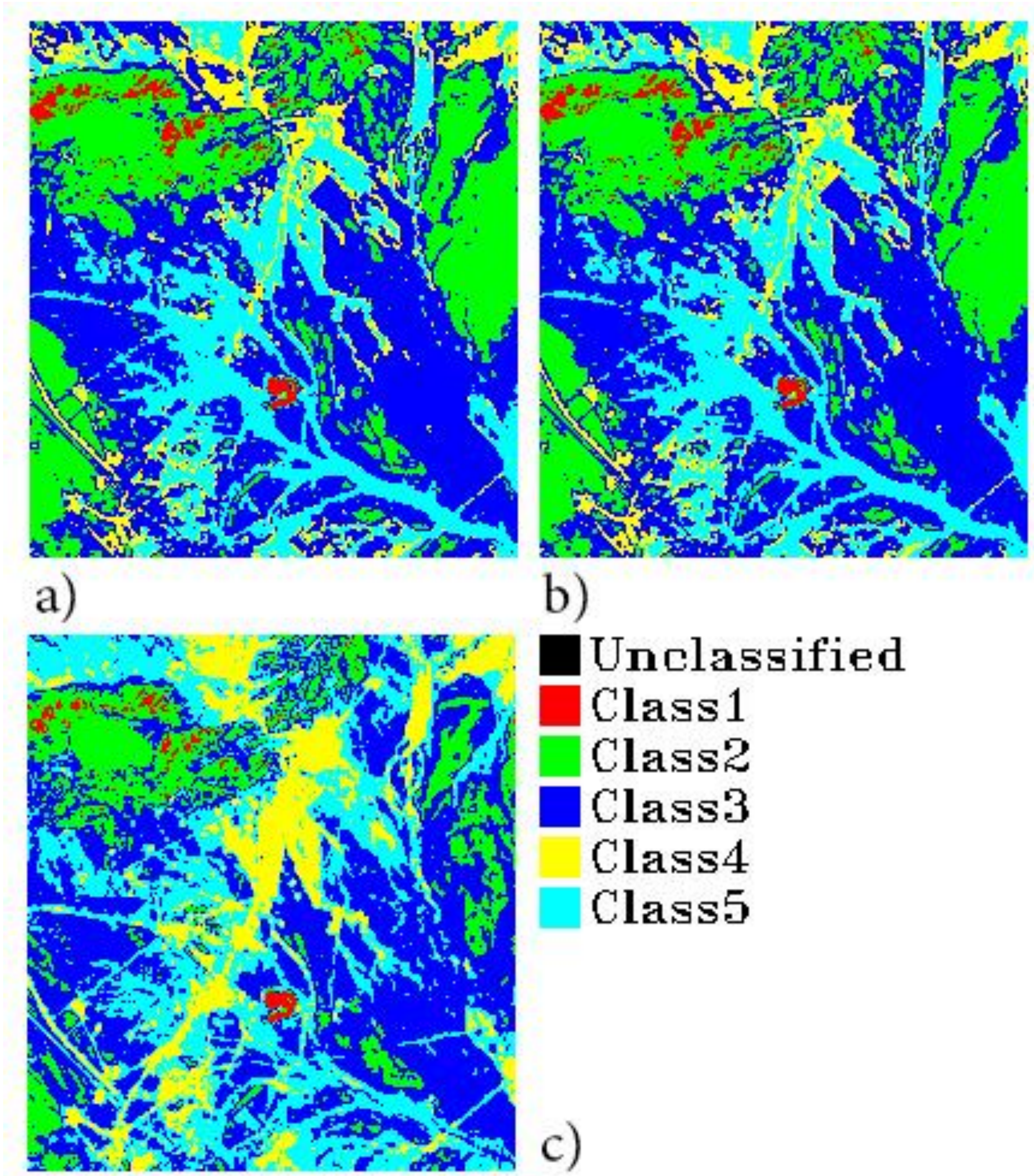

Figure 2. Classification results (red-mining area, green-bedrock, blue-soil, yellow-dirt road, cyan-bare soil) a) Image created by the PCA method b) Image created by high correlation bands clustering d) Image created by defined average of the bands

5. REFERENCES

Amarsaikhan, D. and Ganzorig, M., 1999. Different approaches in feature extraction for hyperspectral image classification. In: Proceedings of the 20th Asian Conference on RS, Hong Kong, pp.434-438.

Amarsaikhan, D., Blotevogel, H.H., van Genderen, J.L., Ganzorig, M., Gantuya, R. and Nergui, B., 2010. Fusing high resolution TerraSAR and Quickbird images for urban land cover study in Mongolia. International Journal of Image and Data Fusion, Vol.1, No.1, pp.83-97.

Amarsaikhan, D., Enkhmanlai, A., Bayarbaatar, D. and Enkhjargal, D., 2011. Classification of hyperspectral images of Mongolia. Informatics, No.11, pp.1-8.

Jia, X., Richards, J.A. and Ricken, D. E., 1999. Remote sensing digital image analysis: an introduction. Berlin: Springer-Verlag.

Keshava, N. and Mustard, J.F., 2002. Spectral unmixing. IEEE Signal Processing Magazine, 19, pp.44 – 57.

Kruse, F.A., 2002, Comparison of AVIRIS and Hyperion for hyperspectral mineral mapping, 11th JPL Airborne Geoscience Workshop, 4-8 March 2002, Pasadena, California.

Plaza, A., Benediktsson, J.A., Boardman, J.W. and Brazile, D., 2009. Recent advances in techniques for hyperspectral image processing. Remote Sensing of Environment, 113, pp.110–122.

Pohl, C., and Van Genderen, J. L., 1998. Multisensor image fusion in remote sensing: concepts, methods and applications. International Journal of Remote Sensing, 19, 823–854.

Richards, J. A., 2005. Analysis of remotely sensed data: The formative decades and the future. IEEE Transactions on Geoscience and Remote Sensing, Volume 43, pp.422 – 432.

Richards, J. A. and Xia, S., 1999. Remote Sensing Digital Image Analysis—An Introduction, 3rd edn (Berlin: Springer-Verlag).

Tsai, F., Lin, E.K. and Yoshino, K., 2007. Spectrally segmented PC analysis of hyperspectral imagery for mapping invasive plant species. International Journal of Remote Sensing, Volume 28, Issue 5, pp.1023-1039.

Vega, D.LS.H and Manian, V., 2012. Object segmentation in hyperspectral images using active contours and graph cuts. International Journal of Remote Sensing, Volume 33, Issue 4, pp.1246-1263.

Yang, C., Everitt, J.H. and Johnson, H.B., 2009. Applying image transformation and classification techniques to airborne hyperspectral imagery for mapping Ashe juniper infestations. International Journal of Remote Sensing, Volume 30, Issue 11, pp.2741-2758.